Human-Humanoid Haptic Joint Object Transportation Case Study

Antoine Bussy, Abderrahmane Kheddar, André Crosnier, François Keith

Human-Humanoid Haptic Joint Object Transportation Case Study

Antoine Bussy[1]   Abderrahmane Kheddar[1,2]   André Crosnier[1]   François Keith[1,2]

Abstract— In this paper, we propose a control scheme that allows a humanoid robot to perform a transportation task jointly with a human partner. From the study of how human dyads achieve such a task, we have developed a control law for physical interaction that unifies standalone and collaborative (leader and follower) modes for trajectory-based tasks. We present it in the case of a linear impedance controller but it can be generalized to more complex impedances. Desired trajectories are decomposed into sequences of elementary motion primitives. We implemented this model with a Finite State Machine associated with a reactive pattern generator. First experiments conducted on a real HRP-2 humanoid robot assess the overall approach.

I. INTRODUCTION

Haptic human-robot joint actions or physical human-robot interaction (pHRI) skills are among the most challenging behaviors to program on a robot. Such haptic joint actions can be classified into: (i) tasks implying close or direct contact (touch) between the human and the robot such as dancing [1], human motion assisting or guiding [2], etc., or (ii) tasks implying indirect contact through an object manipulated by both the human and the robot. In both cases, the robot acts as a *partner* for the human operator. Examples of these can be found in industry, namely in flexible SME or in production line, e.g. [3], but also in collocated spaces such as homes, offices, etc. Obviously, the main challenge is to gain a perfect synergy and complementary, mutual understanding and responsibility sharing in the achievement of the tasks by the human-robot dyad. This challenge must operate under very hard constraints of safety and robustness of the haptic interaction [4][5].

In this paper, we are interested in haptic joint actions for a particular class of robots: *humanoids*. Of course, achieving haptic joint actions with humanoid robots share similar fundamental concerns with any robot such as the ability to understand human intentions from multi-modal sensing, human-in-the-loop motion planning, stable and robust control under safety constraints, etc. Yet, the anthropomorphic resemblance with human offers distinguishing investigations relatively to fixed-base or wheeled robots, for example:

- the reactivity planning in the generation of footprints and whole-body motion in close contact with a human whatever the walking phase in progress is;
- coordinating locomotion and manipulation under equilibrium and haptic task constraints. For example, the humanoid's arms can play several roles: absorb excess of (internal) forces, smooth the motion of the object and

accompany its motion during walking, smooth changes in walking directions, etc.

In Section II we investigate how a human dyad performs the transportation task. Based on this investigation, we present a control scheme structured in two parts. The first part is a trajectory-based control law for physical interaction that encompasses the realization of the task alone or with a partner, and is described in Section III. The second part is a motion predictor of the partner intentions that relies on a decomposition of the motion in elementary primitives. It is described in Section IV. We test our control scheme in Section V by making our HRP-2 humanoid robot perform the task with a human partner.

II. HUMAN DYAD EXPERIMENTS

We studied how a human dyad jointly performs the task of our interest: beam transportation. We monitored the subjects' postures with a motion capture system, as well as the forces and moments they exert on the object.

A. Task and Scenarios

The task we studied is a locomotion task in which the subjects move a table-like object over a few meters –one subject walks backwards, the other forwards– and move back to the initial position.

We defined three scenarios with different role assignments:

- No role assignment (Free)
- Subject 1 is leader, subject 2 is follower (1L2F)
- Subject 1 is follower, subject 2 is leader (1F2L)

The different assignments were always acquired in this order so that the subjects would not be spoken of role assignment for the no-role-assignment scenario. The start signal of the task was vocally given by the experimenter in the first scenario, and was left to the appreciation of the leader in the two last.

B. Data Acquisition System

The subjects' postures were acquired using a Vicon Work-Station 624 system with five MCam2 cameras. An overall of 40 passive markers of 8 millimeters of diameter –18 and 19 for the two subjects and 3 for the object– were used. The trajectories of the markers were sampled at 100Hz.

The table-like object was specifically designed for the experiment, as we needed the force-torque sensors to be mounted on it. Moreover, it had to be as non-obstructive as possible in order not to hide the markers of the inferior part of the subjects' bodies from the cameras. The experimental setup is shown in Fig. 1.

[1]Université Montpellier 2-CNRS, LIRMM, Interactive Digital Human group, 161 rue Ada, F-34095, Montpellier cedex 5, France. Contact: <name>@lirmm.fr
[2]CNRS-AIST Joint Robotics Laboratory UMI3218/CRT, Tsukuba, Japan.
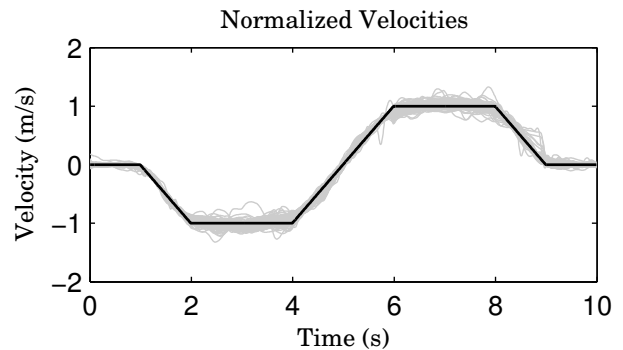
Fig. 1. Experimental setup.

Fig. 2. Observed Normalized Velocities (in gray) and a trapezoidal approximation (in black). Velocities were normalized so that they all have the same trapezoidal approximation.

C. Subjects

We acquired data with sixteen healthy subjects (eight dyads), aged 14-32 (mean 25), four female, twelve male, fifteen right-handed, one mixed-handed. For every dyad, we acquired each couple scenario five times, which gives a total of fifteen acquisitions by dyad.

D. Trajectory-based Task

As in our previous work [6], we observed that the main invariant of the task was the object trajectory in the operational frame, even in a collaborative task. The trajectory can be decomposed in Constant Velocity Phases (CVPs). In each trial, two of these phases are observed : one forwards, the other backwards. If the zero-velocity phases are taken into account, the object's velocity profile can thus be decomposed in four CVPs: zero, forwards, backwards, zero. These phases are separated by rise transition phases we approximate as affine functions of time, which leads to a trapezoidal approximation of the object's velocity.

To support our observation, we fitted all the object's velocities from our data with a four CVP decomposition, as shown in Fig. 2. We identified the forwards and backwards velocities (2 parameters) and the phases switch moments (6 parameters). All velocity profiles were fitted with a mean correlation coefficient of 0.997 (standard deviation: 0.0019).

Note that different successions of CVPs could produce various motions, which makes the CVPs a set of *motion primitives*, i.e. a set of elementary motions.

Contrariwise, such an invariant could not be as easily observed in forces applied by the subjects on the object. These observations stress that the object trajectory is predominant in defining our transportation task and therefore should be taken into account in the design of our control law. However, it might not be the case for other tasks that would require more force and/or dexterous manipulation.

III. UNIFIED CONTROL LAW FOR pHRI

Throughout this paper, we only consider a task along one degree of freedom. Thus, gravity and orientation do not appear in the dynamic equations. We generalize our approach to several degree of freedom in [7]. Besides the robot firmly

holds the object, therefore the robot's hands trajectories and the object trajectory only differ by a constant vector and controlling the object's position is equivalent to controlling the robot's hands'. We make no distinction between the two in the following.

A. Desired features

We aim at designing a low level control law for physical interaction with the following characteristics:

- it can be used for both standalone and collaborative modes (leader and follower);
- it should be able to accurately perform any desired trajectory x_d of the object in standalone mode without perturbation while insuring safe interaction in case of contact with the environment.

These characteristics are based on the assumptions that the human being

- does not behave very differently when performing the task alone or collaboratively as a leader or a follower;
- is able to perform accurately an intended Cartesian trajectory when transporting an object alone.

Let's take an example. Consider a transportation task – performed alone or in collaboration– where a third person punctually hits the hand of one of the manipulators. We claim that the effect caused by this disturbance on the hand should be the same regardless of the mode –standalone, collaborative leader, collaborative follower.

B. Proposed Control Law

Based on the *equilibrium trajectory hypothesis* [8], we propose a simple trajectory-referenced admittance control law [9]:

$$F = -b\dot{x} + k(x_0 - x) \qquad (1)$$

where:

- x is the object trajectory,
- x_0 is the input equilibrium trajectory,
- F is the force applied by the manipulator on the object,
- b and k are damping and stiffness coefficients.

In standalone mode, where the only force applied on the object is F, we have

$$m\ddot{x} = F = -b\dot{x} + k(x_0 - x) \qquad (2)$$

where m is the object mass. The trajectory x_0 is generally not reached –i.e. is not a solution of (2) –and is thus referred as *virtual* by Hogan [9]. We choose

$$x_0 = \frac{1}{k}(m\ddot{x}_d + b\dot{x}_d + kx_d). \tag{3}$$

where x_d is supposed to be twice continuously differentiable. Equation (2) becomes

$$m(\ddot{x} - \ddot{x}_d) + b(\dot{x} - \dot{x}_d) + k(x - x_d) = 0 \tag{4}$$

whose solution x converges asymptotically to x_d with stable gains m, b and k. Thus, the admittance control law has an input desired trajectory x_d, as well as a force feedback F from the robot's sensors; it computes the effective trajectory x of the object that will be realized by the robot through position control.

To sum up, if we can correctly predict the dynamics of the object, i.e. its inertia and all the forces exerted on it, we can adapt the equilibrium trajectory x_0 so that the desired trajectory x_d is reached. In our simple case, it only means estimating the object mass m, which can be done at the experiment start-up by measuring the force vertical component. Note that an error of the dynamics prediction would result in an error in x_0 which would be "filtered" by the admittance the same way as an error on x will be.

C. Behavior in Collaborative Mode

Here, we assume that the forces applied by the other partner in collaborative mode cannot be predicted. Thus, the method used previously cannot be repeated. However, we show that there is an alternative method to achieve a desired trajectory. We also assume that both partners are able to share the load of the object dynamics. In our simple case, there is only the object predicted inertia $m\ddot{x}_d$, i.e. the object mass. As the partners are sharing the object weight, they can assume the inertia of the portion of the object they are carrying. In the following, we assume an equal sharing of $m/2$ for simplicity. All the reasoning described in this subsection can be straightforwardly extended to several partners. The notations of the previous subsection are reused, indexed with the number of the partner $i \in \{1,2\}$.

Applying (2) and (3) for each partner, we obtain the following object dynamic equation

$$m\ddot{x} = \sum_{i=1}^{2} \frac{m}{2}\ddot{x}_{d,i} + b_i(\dot{x}_{d,i} - \dot{x}) + k_i(x_{d,i} - x) \tag{5}$$

In this equation, we assume that the second partner control law is the one we propose for clarity's sake, but it is only necessary for $x_{d,2}$ to be the solution of

$$\frac{m}{2}\ddot{x} = F_2(x) \tag{6}$$

i.e. the second partner is able to perform accurately a desired trajectory when transporting half the object alone. In the case where

$$x_{d,1} = x_{d,2} = x_d \tag{7}$$

the realized trajectory is x_d and $F_1 = F_2 = m\ddot{x}_d/2$ which is the equal sharing of the task. In practice, we would rather have

$$\begin{cases} \dot{x}_{d,1} = \dot{x}_{d,2} = \dot{x}_d \\ x_d = \dfrac{k_1 x_{d,1} + k_2 x_{d,2}}{k_1 + k_2} \end{cases} \tag{8}$$

The position offset between $x_{d,1}$ and $x_{d,2}$ will result in a constant co-contraction force between partners which is observed in [10] as well as in our experimental data.

Thus, in order to achieve an equal sharing of the task, both partners should have the same desired trajectory [11]. Otherwise, different desired trajectories will result in unnecessary forces exerted by the two partners. These statements are already well-known and predicting a human partner's desired trajectory is one of the main challenges in the pHRI field. However, how x_d is determined is completely independent of our control law, so that it can be used in both standalone and collaborative modes. The difference between these modes lies in the trajectory planning of x_d. In the standalone mode, a preplanned trajectory could be used in the simplest case. In a leader control law, we could also use a preplanned trajectory. However, the desired trajectory should always be adapted according to the follower's reactions, in the situation where the latter needs to stop because s/he's losing balance for instance. In a follower control law, the desired trajectory should be the prediction of the leader intended trajectory.

More importantly, assuming we have trajectory planners for each of the three modes, it is possible to switch the robot behavior as theorized in [11][12] by switching the planners, without changing the control law that regulates the physical interaction.

IV. FOLLOWER TRAJECTORY PLANNER

In this part, we propose a basic trajectory planner for the follower mode based on observations made in Section II. Other modes are left for future work.

A. Motion Primitives

As stated previously, planning a trajectory in a follower mode consists in predicting the leader's intended trajectory. Motion prediction of the human partner has been addressed throughout the literature in pHRI. The strategy generally aims at reducing the problem to the estimation of a handful parameters that allows to generate a complete motion. The most famous example is the minimum jerk model [13]. However this model is always applied to the overall motion and does not fit for motions over large distances. That is why we suggest to decompose the motion in phases, as it had been addressed for handshaking [14] and dancing [15], and as our experiment with human subjects suggests. The CVP decomposition we introduced defines two classes of *motion primitives*:

- stay at velocity V during T seconds (stationary)
- change to velocity V in T seconds (transition)

Thus, each motion primitive can be parametrized with two numbers in the case of a one-degree-of-freedom motion. Composing different sequences of these primitives can

produce various motions. For instance, if we set the time parameter T aside, the motions of Fig. 2 can be described by the following sequence:

- start at velocity 0
- change to velocity V
- stay at velocity V
- change to velocity $-V$
- stay at velocity $-V$
- change to velocity 0

For any such sequence, we need to generate a full motion at each instant t with an interpolation method. To obtain smooth trajectories, as they should be performed in standalone mode, we chose to use step-responses of the following critically-damped second order system to compute the desired velocity v_d

$$\ddot{v}_d + 2\omega_0 \dot{v}_d + \omega_0^2(v_d - V) = 0 \qquad (9)$$

where ω_0 can easily be computed from T. Finally the full planned motion x_d is obtained by integrating v_d.

This method is not specific to the follower mode. A sequence of primitives can also be used to describe a desired trajectory for the standalone and leader modes. However this approach greatly simplifies the estimation of the leader intentions in the follower mode. A parallel can be established with speech recognition where primitives would be words and the complete motion would be a sentence.

B. Reactive Generation of Primitives Sequences

With our choice of primitives, we have two parameters T and V to estimate. But more importantly, we need to determine the switch timings from one primitive to the next. We will focus on the latter point. We will therefore consider T constant as a simplification, typically about one second. This means that our robot will not be able to adapt its acceleration. Thus we only need to generate a value for V at each instant t.

It is important to note that fixing T does not mean that V will be necessarily constant over phases of T seconds, as a motion primitive can be interrupted by the detection of an event. For example, consider the situation where the follower is planning a constant velocity V for the next T seconds, based upon his/her prediction of the leader intentions. Before this time lap elapses, the leader decides to brake. The follower should brake as soon as s/he detects this event, regardless of the parameter T.

To detect the switch timings and generate the values of V, we designed a Finite State Machine (FSM) with four states based on the trapezoidal approximation of Fig. 2. The purpose of the FSM is mainly to determine the switch timings between the zero-velocity primitive and the other ones by detecting accelerating and braking events. The major issue is to distinguish the intention to brake of the human partner from the intention to just slow down. For the sake of clarity, we describe our strategy for positive velocities.

- **0:** The zero-CVP state (and initial state), where $V = 0$. When the velocity v of the object exceed a threshold, V is set to $V_{default}$ and the FSM enters the next state **TV**.

- **TV:** The acceleration state, where $V = V_{default}$. After T seconds, V is set to the current object velocity v and the FSM enters the next state **V**.
- **V:** The CVP state, where V is updated every T seconds to the current object velocity v. When $V - v$ falls below a threshold V is set to zero and the FSM enters the next state **T0**.
- **T0:** The braking state, where $V = 0$. After T seconds, the FSM enters the first state **0**.

The transitions are triggered by the object velocity v and the time δt spent in the current state. Apart from thresholds, two constant parameters are used in the FSM, T and $V_{default}$. T is the time parameter previously defined. $V_{default}$ should be an estimation of the desired target velocity of the leader, but it is chosen constant in the implementation presented in this article. From human-human experimental data, it should be about 0.6 m/s. Given the limited walking capabilities of our robot, it was set to 0.2m/s.

More generally, the FSM lacks an estimator of the value of non-zero-velocity primitives, although it can determine its sign. Here, we rely on the hypothesis that, most of the time, the leader updates its desired velocity to the object velocity if the one s/he planned is not realized. Thus, if the robot adapts its desired velocity while in the state **V** by updating it every T seconds with the object current velocity, the leader's and robot's intended velocity quickly converge. Otherwise, if the leader chooses not to adapt, the FSM progressively updates the robot's desired velocity with a higher one until it reaches the leader's plan.

The present FSM reactively generates motion primitives for a follower mode. Though it roughly estimates the leader's intentions, it allows us to test the proposed control scheme on our HRP-2 humanoid robot.

C. Velocity-triggered transitions

The transitions of our FSM are triggered by threshold detection on the object velocity v (or $\dot{x}$) computed by solving (1) with force measurements from the robot's sensors at its wrists. We choose velocity thresholds over force thresholds because we describe the task with velocity. Each state of the FSM is associated with a given velocity, which is not possible with forces because of internal forces. A too important error between the velocity from the FSM and the object actual velocity indicates that the FSM needs a state update and therefore triggers a transition.

V. IMPLEMENTATION AND EXPERIMENTATION ON THE HRP-2 HUMANOID ROBOT

The proposed control scheme is globally described in Fig. 3. We will detail the different components in the following parts.

A. Physical Interaction and Locomotion

The HRP-2 humanoid robot interacts with its environment through two force-torque sensors mounted on each wrist that measured two forces F_L and F_R, that we sum to get the force feedback F for the admittance controller. The stiffness k and
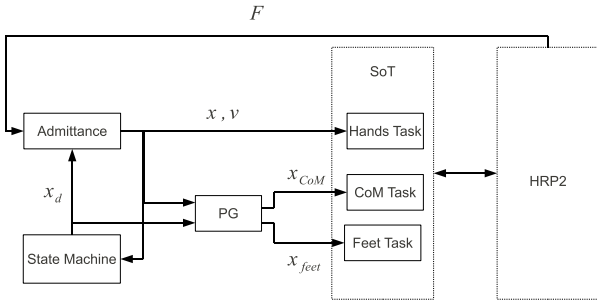
Fig. 3. The Complete Control scheme.

damping b coefficients were experimentally tuned ($k_{xy} = 40$, $b_{xy} = 85$, $k_z = 250$, $b_z = 200$). The admittance controller computes the trajectory x of the robot's hands in the world frame. The state machine uses this trajectory to compute a reactive trajectory plan X and then the desired trajectory x_d. The hands are position-controlled through the Stack of Tasks (SoT) developed in [16]. The SoT allows to define various tasks –positioning the hands in the world frame in our case– and uses the robot redundancy to realize them simultaneously.

For the locomotion, we used the walking Pattern-Generator (PG) developed in [17]. The PG generates on-line a trajectory for the Center of Mass (CoM) of the robot as well as trajectories for the feet, that are also executed through the SoT.
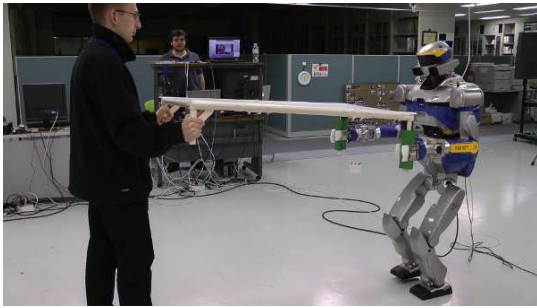
B. Results

Fig. 4. HRP-2 realizing the transportation task as a proactive follower with a human partner.

As pictured in Fig. 4 and in the attached video, our robot successfully performed the task with a human leader, though at limited velocity. Trajectories x, x_d, x_0 and X are shown in Fig. 5. Their corresponding velocities are shown in Fig. 6. The trapezoidal velocity profile of Fig. 2 was reproduced and the robot correctly detected the start, move-back and stop of the motion. Besides, we can observe that the error between the desired and equilibrium trajectories x_d and x_0 is not small (about 0.3m), which validates the necessity to compute x_0 from (3) instead of setting $x_0 = x_d$.

If we look at the force in Fig. 7, we can see that the initial and final forces are not zero. Unlike a passive impedance controller, our control scheme successfully reproduces the co-contraction force reported by Reed [10] and which also appears in our human-dyad experiments. Most of the time, our control law results in forces that counteract the motion, whereas it is always the case for the passive control law. However, when the motion starts, our control law quickly produces less forces, especially when the object effective and desired velocities are the same, where the force come back to the co-contraction initial value. During constant velocity phases, for any velocity, the human partner can exert the force s/he feels comfortable with, without affecting the task execution. The more important force variations occur during the transition phases, which only represents a small part of the overall motion.

Oscillations can be observed in the velocity profile in Fig. 6; we do not precisely investigate their origin. We suspect they might be caused by the robot stepping. Nonetheless they do not destabilize the pHRI control. On the video, we can also notice that the feet are sliding, which might also contribute to emphasize the oscillations.
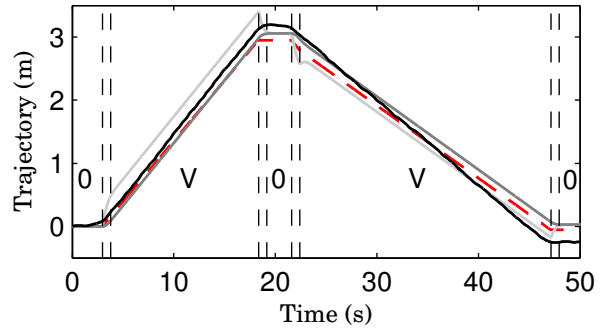

Fig. 5. Trajectories of the object: the admittance controller output x in black, follower desired trajectory x_d in dark gray, equilibrium trajectory x_0 in light gray, motion primitives X in dotted red (integral of V). The switch timings of the FSM are represented by vertical dotted black lines. The transition states **TV** and **T0** are not represented.

VI. DISCUSSION AND CONCLUDING REMARKS

In this paper, we proposed a complete control scheme that allows our HRP-2 robot to perform a transportation task with locomotion, jointly with a human partner.

The first main contribution is a control law for physical interaction that unifies standalone and collaborative (leader and follower) modes for trajectory-based tasks. Although we presented it for a simple impedance controller, it can be generalized to more complex impedances – e.g. non-linear.

The second important contribution is the decomposition of a trajectory in a few motion primitives that allows to succinctly describe a large diversity of motions. The example we described and implemented is but a simple one. It can be made more complex with additional primitives to widen the possible motions and tasks. We are thinking about primitives that allow precise positioning of the manipulated object, which we are not considering in our transportation task. Nevertheless, adding more primitives also complexifies the design of a reactive generator of primitives sequences.

Several other improvements could be brought to our design. For instance, our FSM could be replaced by a
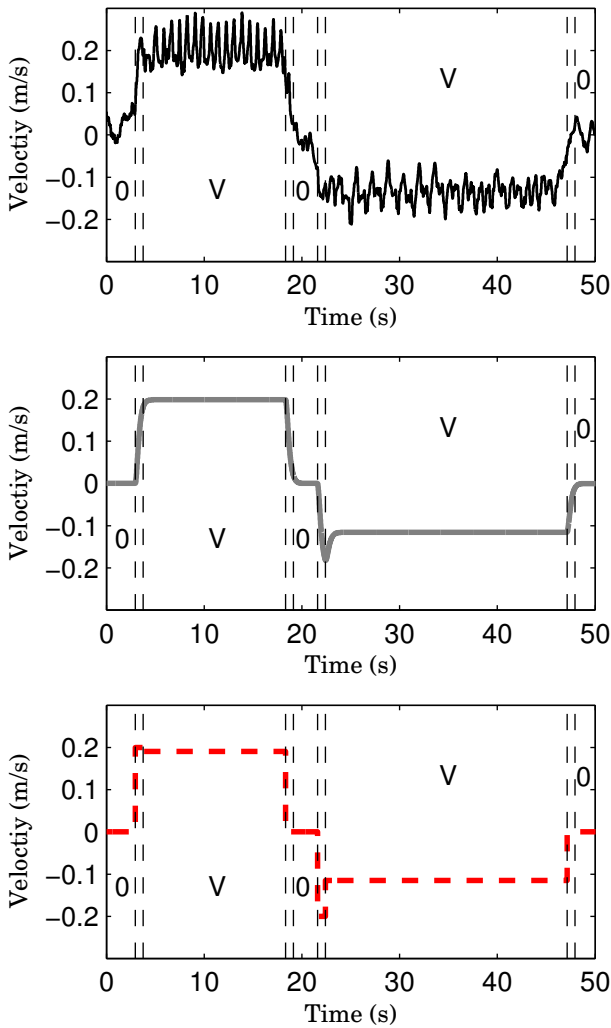
Fig. 6. Velocities of the object: the admittance controller output v in black (top), follower desired velocity v_d in gray (middle), motion primitives V in dotted red (bottom). The switch timings of the FSM are represented by vertical dotted black lines. The transition states **TV** and **T0** are not represented.
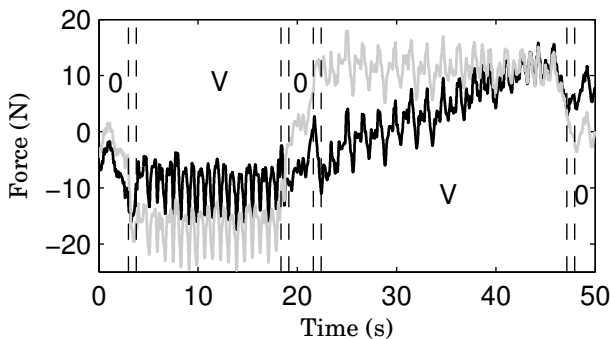

Fig. 7. Force applied by the robot on the object (black). The gray curve represents the damping part of the interaction force $F = -b\dot{x}$: it is the force that would be applied by the robot with a passive behavior. The switch timings of the FSM are represented by vertical dotted black lines. The transitions states **TV** and **T0** are not represented.

Hidden Markov Model (HMM). The interpolation method

from the primitive parameters to the full motion phase could also be improved. A polynomial interpolation may yield better results: the minimum jerk trajectory would be a very reasonable choice as in [13]. We found in [6] that phase decomposition coupled to minimum jerk interpolation on each phase tended to better describe the motion than a minimum jerk interpolation on the overall motion.

REFERENCES

[1] K. Kosuge, T. Hayashi, Y. Hirata, and R. Tobiyama, "Dance partner robot –Ms DanceR–," in *IEEE/RSJ International Conference on Robots and Intelligent Systems*, October 2003, pp. 3459–3464.
[2] O. Khatib, *Object manipulation in a multi-effector robot system*. Cambridge: MIT Press, 1988, ch. Robotics Research 4, pp. 134–144.
[3] J. R. Medina, M. Lawitzky, A. Mörtl, D. Lee, and S. Hirche, "An experience-driven robotic assistant acquiring human knowledge to improve haptic cooperation," in *IEEE/RSJ International Conference on Intelligent Robots and Systems (IROS)*, 25-30 September 2011.
[4] V. Duchaine and C. Gosselin, "Safe, stable and intuitive control for physical human-robot interaction," in *IEEE International Conference on Robotics and Automation*, 12-17 May 2009, pp. 3383–3388.
[5] S. Haddadin, A. Albu-Schäffer, and G. Hirzinger, "Requirements for safe robots: Measurements, analysis and new insights," *The International Journal of Robotics Research*, vol. 28, no. 11-12, pp. 1507–1527, November/December 2009.
[6] S. Miossec and A. Kheddar, "Human motion in cooperative tasks: Moving object case study," in *IEEE International Conference on Robotics and Biomimetics*. IEEE, February 2008, pp. 1509–1514.
[7] A. Bussy, P. Gergondet, A. Kheddar, F. Keith, and A. Crosnier, "Proactive behavior of a humanoid robot in a haptic transportation task with a human partner," in *21th IEEE Int. Symposium on Robot and Human Interactive Communication (Ro-Man 2012)*, September 2012.
[8] T. Flash, "The control of hand equilibrium trajectories in multi-joint arm movements," *Biological Cybernetics*, vol. 57, pp. 257–274, 1987.
[9] N. Hogan, "Impedance control: an approach to manipulation," *Journal of Dynamic Systems, Measurement, and Control*, vol. 107, pp. 1–24, March 1985.
[10] K. B. Reed, "Understanding the haptic interactions of working together," Ph.D. dissertation, Northwestern University, Evanston, Illinois, USA, June 2007.
[11] A. Kheddar, "Human-robot haptic joint actions is an equal control-sharing approach possible?" in *IEEE International Conference on Human System Interactions (HSI)*, 19-21 May 2011, pp. 268–273.
[12] P. Evrard and A. Kheddar, "Homotopy switching model for dyad haptic interaction in physical collaborative tasks," in *Joint EuroHaptics Conference and Symposium on Haptic Interfaces for Virtual Environment and Teleoperator Systems*. IEEE, March 2009.
[13] B. Corteville, E. Aertbelien, H. Bruyninckx, J. D. Schutter, and H. V. Brussel, "Human-inspired robot assistant for fast point-to-point movements," in *IEEE International Conference on Robotics and Automation*. Roma, Italy: IEEE, April 2007, pp. 3639–3644.
[14] Z. Wang, A. Peer, and M. Buss, "An hmm approach to realistic haptic human-robot interaction," in *Joint EuroHaptics Conference and Symposium on Haptic Interfaces for Virtual Environment and Teleoperator Systems*. IEEE, March 2009, pp. 374–379.
[15] T. Takeda, Y. Hirata, and K. Kosuge, "Hmm-based error recovery of dance step selection for dance partner robot," in *IEEE International Conference on Robotics and Automation*. IEEE, April 2007, pp. 1768–1773.
[16] N. Mansard, O. Stasse, P. Evrard, and A. Kheddar, "A versatile generalized inverted kinematics implementation for collaborative humanoid robots: The stack of tasks," in *IEEE Internationl Conference on Advanced Robotics*, Munich, Germany, June 2009.
[17] A. Herdt, N. Perrin, and P.-B. Wieber, "Walking without thinking about it," in *IEEE/RSJ International Conference on Intelligent Robots and Systems (IROS)*, 2010, pp. 190–195.